



Original Articles

Histamine receptor 1 inhibition enhances antitumor therapeutic responses through extracellular signal-regulated kinase (ERK) activation in breast cancer



Patricia Fernández-Nogueira ^{a, b, 1}, Aleix Noguera-Castells ^{a, b, 1}, Gemma Fuster ^{a, b},
 Leire Recalde-Percaz ^{a, b}, Núria Moragas ^{a, b}, Anna López-Plana ^{a, b}, Estel Enreig ^{a, b},
 Patricia Jauregui ^{a, b}, Neus Carbó ^c, Vanessa Almendro ^{a, b}, Pedro Gascón ^{a, b, c, d},
 Paloma Bragado ^{a, b, **, 1}, Mario Mancino ^{a, b, *, 1}

^a Institut d'Investigacions Biomèdiques August Pi i Sunyer (IDIBAPS), Barcelona, Spain

^b Department of Medicine, University of Barcelona, Barcelona, Spain

^c Department of Biochemistry and Molecular Biomedicine, University of Barcelona, Barcelona, Spain

^d Department of Medical Oncology, Hospital Clínic, Barcelona, Spain

ARTICLE INFO

Article history:

Received 18 January 2018

Received in revised form

7 March 2018

Accepted 12 March 2018

Keywords:

Breast cancer

Histamine receptor 1

Microenvironment

Neuropeptide

Terfenadine

Apoptosis

ABSTRACT

Histamine receptor 1 (HRH1) belongs to the rhodopsin-like G-protein-coupled receptor family. Its activation by histamine triggers cell proliferation, embryonic development, and tumor growth. We recently established that HRH1 is up-regulated in basal and human epidermal growth factor receptor 2 (HER2)-enriched human breast tumors and that its expression correlates with a worse prognosis. Nevertheless, the functional role of HRH1 in basal and HER2-targeted therapy-resistant breast cancer (BC) progression has not yet been addressed. Using terfenadine, a selective chemical inhibitor of HRH1, we showed that the inhibition of HRH1 activity in basal BC cells leads to sub-G0 cell accumulation, suppresses proliferation, promotes cell motility and triggers the activation of extracellular signal-regulated kinase (ERK) signaling, initiating the mitochondrial apoptotic pathway. Furthermore, HER2-targeted therapy-resistant cells express higher levels of HRH1 and are more sensitive to terfenadine treatment. Moreover, *in vivo* experiments showed that terfenadine therapy reduced the tumor growth of basal and trastuzumab-resistant BC cells. In conclusion, our results suggest that targeting HRH1 is a promising new clinical approach to consider that could enhance the effectiveness of current therapeutic treatment in patients with basal and BC tumors resistant to HER2-targeted therapies.

© 2018 The Authors. Published by Elsevier B.V. This is an open access article under the CC BY-NC-ND license (<http://creativecommons.org/licenses/by-nc-nd/4.0/>).

Introduction

Despite significant research advances, cancer remains a worldwide health problem with high related mortality [1]. Breast cancer (BC) is the second leading cause of cancer death in women after

lung cancer [2]. BC is a heterogeneous disease, and insights from genomics have led to the identification of five molecular subtypes of BC according to gene expression patterns: luminal A, luminal B, human epidermal growth factor receptor 2 (HER2)-enriched, basal and claudin low [3,4]. These have different clinical outcomes and responses to chemotherapy: luminal A tumors have the highest overall, breast-specific, or relapse-free survival rate. In general, luminal B is associated with intermediate prognosis, and basal tumors have the lowest survival rate, principally due to the lack of suitable molecular targeted therapies. Outcomes for women diagnosed with HER2-enriched cancer have improved greatly in recent decades due to the use of HER2-targeted therapies [5,6]. However, resistance and the failure of therapies to cure metastatic BC have reduced their success [7], making necessary the discovery of novel

* Corresponding author. Laboratory of Molecular and Translational Oncology, CELLEX - Centre de Recerca Biomèdica - Laboratori 1A, C/Casanova 143, 08036, Barcelona, Spain. Tel.: 0034 93 227 54 00x4801//4013.

** Corresponding author. Laboratory of Molecular and Translational Oncology, CELLEX - Centre de Recerca Biomèdica - Laboratori 1A, C/Casanova 143, 08036, Barcelona, Spain. Tel.: 0034 93 227 54 00x4801//4013.

E-mail addresses: bragado@clinic.cat (P. Bragado), mmancino@clinic.cat (M. Mancino).

¹ These authors contributed equally to this work.

therapies targeting different mechanisms of action to improve outcomes.

Pro-inflammatory cytokines, growth factors, angiogenesis- and lymphangiogenesis-inducing factors and immune factors are the best-characterized soluble microenvironmental factors regarding their contribution to tumor progression [8]. However, the presence of nerve endings within tumors has been described in several cancers [9–11], and cancer cells express receptors for neuropeptides and neurotransmitters [12] that have been shown to stimulate migration, promote tumor growth and affect the chemotherapeutic response of cancer cells [13]. In the last decade, our group and others have demonstrated that the nervous system and nerve-related factors play an important role in cancer progression and dissemination [14–16]. In addition, two pioneering studies in prostate [17] and gastric [18] cancer have shown that peripheral nerves are an essential component of the tumor microenvironment and regulate cancer progression and metastasis. Indeed, we have recently identified a set of neurogenes that are expressed differently between BC subtypes and whose expression correlates with the prognosis [14]. Among them, we found the neurogene histamine receptor 1 (HRH1) to be up-regulated in basal and HER2-enriched tumor samples [14]. Over-expression of HRH1 in cancer has been reported by other authors [19]. In experimental mammary carcinomas, histamine becomes an autocrine growth factor that regulates cell proliferation via HRH1 and histamine receptor 2 (HRH2), as one of the early events responsible for the onset of malignant transformation. *In vivo* treatment with HRH2 antagonists produced complete remission in 70% of experimental tumors [20–22]. However, the role of HRH1 in basal BC progression and resistance to HER2-targeted therapies has not been addressed until now.

HRH1 mediates the functional effects of histamine in multiple cell types through activation of the $G\alpha_q/11$ heterotrimeric G protein and its downstream effector, phospholipase C (PLC). PLC breaks down phosphatidylinositol 4,5-bisphosphate to inositol 1,4,5-trisphosphate (IP3) and 1,2-diaclyglycerol. IP3 acts on specific receptors in the endoplasmic reticulum (ER) membrane and mobilizes Ca^{2+} from ER reserves, activating certain proteins, including extracellular signal-regulated kinase (ERK), that are involved in cell proliferation and survival [23–25].

Terfenadine, an HRH1 antagonist formerly used for the treatment of allergic conditions [26], has been shown to exert growth-inhibitory effects and apoptotic activity against neoplastic mast cells [27] and melanoma cells [28] through disturbance of intracellular calcium homeostasis, caspase 2 activation and the mitochondrial pathway of caspase 9 activation. However, the exact signaling pathway that explains the anti-cancer activity of terfenadine, particularly in BC, remains unclear.

The aim of this study was to determine the effects of HRH1 inhibition by terfenadine on the development and progression of basal BC and on BC cells resistant to HER2-targeted therapies.

We provide evidence that, in these BC cell subtypes, HRH1 inhibition triggers the activation of ERK signaling, which then initiates the mitochondrial apoptotic pathway and caspase cascade activation, culminating in the apoptotic death of basal BC cells and BC cells resistant to trastuzumab and lapatinib. These results underline the therapeutic potential of HRH1 inhibition in these aggressive BC subtypes.

Materials and methods

Cell lines and cultures

Human BC cell lines were obtained from the American Type Culture Collection (ATCC, Manassas, VA, USA) and were cultured in

Dulbecco's Modified Eagle Medium/Nutrient Mixture F-12 (DMEM/F12) (Gibco, Life Technologies, CA, USA; #21331–020), Roswell Park Memorial Institute medium (RPMI) (Gibco, #A10491-01) or DMEM (Gibco, #41966–029) (MCF7) supplemented with 10% fetal bovine serum (Gibco, #10270–106), 5% Glutamax (Gibco, #3550–038) and 5% fungizone-penicillin-streptomycin mixture (Invitrogen, Thermo Fisher Scientific, CA, USA; #15070–063) (hereafter referred to as complete culture medium). They were cultivated in a humidified atmosphere of 5% CO_2 at 37 °C. For the MCF-7, BT-549 and BT-474 cell lines, 10 μ g/ml of insulin (Sigma, MO, USA; #I9278) was added to the media. Trastuzumab- and lapatinib-resistant human BC cells were generated by exposing them to gradually increasing concentrations of lapatinib and trastuzumab for five months, and resistance was tested using cell proliferation assays.

Cell apoptosis assay

For the induction of apoptosis, assay cells were seeded in 6-well culture plates with complete media and were allowed to grow until sub-confluence. The cells were then incubated overnight with serum-free media for synchronization, followed by treatment with terfenadine (Sigma, MO, USA; #T9652) at the half maximal inhibitory concentration (IC50) value for each cell line and 40 μ M PD98059 (MEK1 inhibitor) (Cell Signaling, MA, USA; #9900S) for 48 h. Apoptotic cells were quantified using an Annexin V-fluorescein isothiocyanate (FITC)/propidium iodide (PI) double staining kit (Thermo Fisher, Scientific, CA, USA; #V23200) according to the manufacturer's protocol. Briefly, cells and media were collected and washed with phosphate-buffered saline (PBS; Gibco; #14190–094). Cells were resuspended in binding buffer containing FITC-conjugated annexin V and PI and were incubated for 15 min in the dark. The samples were analyzed by flow cytometry (Fortessa) and were quantified using FACSDiva software (BD Biosciences CA, USA). The cells were classified as follows: alive (Annexin-/PI-), early apoptotic (Annexin+/PI-), late apoptotic (Annexin+/PI+) and necrotic (Annexin-/PI+).

Immunofluorescence

The cells were seeded in glass coverslips until sub-confluence and were synchronized by serum-deprivation overnight. They were then washed twice with PBS and fixed with 0.4% paraformaldehyde (PFA; PanReac, Barcelona, SPAIN; #A3697,500) for 20 min at 4 °C. After being washed three times with PBS, fixed cells were blocked with 3% bovine serum albumin (BSA; SIGMA; A7906) and 2% normal goat serum (NGS; SIGMA; G9023) in PBS for 1 h and were incubated with HRH1 antibody (Santa Cruz Biotechnology, CA, USA; sc20633) overnight at 4 °C. The coverslips were washed three times with PBS and were incubated with the secondary antibody for 1 h at room temperature (RT) (anti-rabbit secondary antibody conjugated with Alexa 488) (Life Technologies; #A11034). After washing three times, nuclei were counterstained with 4',6-diamidino-2-phenylindole (DAPI) (Life Technologies, #H3570) for 10 min, and coverslips were mounted on glass with Prolong Gold Antifade reagent (Life Technologies, P36930). The cells were analyzed using an Olympus Bx41 microscope, and the images were merged and quantified using ImageJ software (NIH, MD, USA).

Western blotting

The cells were seeded in 6-well plates and were grown until 70–80% confluence. The cells were treated with terfenadine at the IC50 dose for each cell line (SIGMA; #T9652), PD98059 40 μ M (Cell Signaling; #9900), SB203580 2.5 μ M (MERCK, NJ, USA; #506153) or Z-VAD 10 μ M (ChemCruz, CA, USA; #SC311561) at

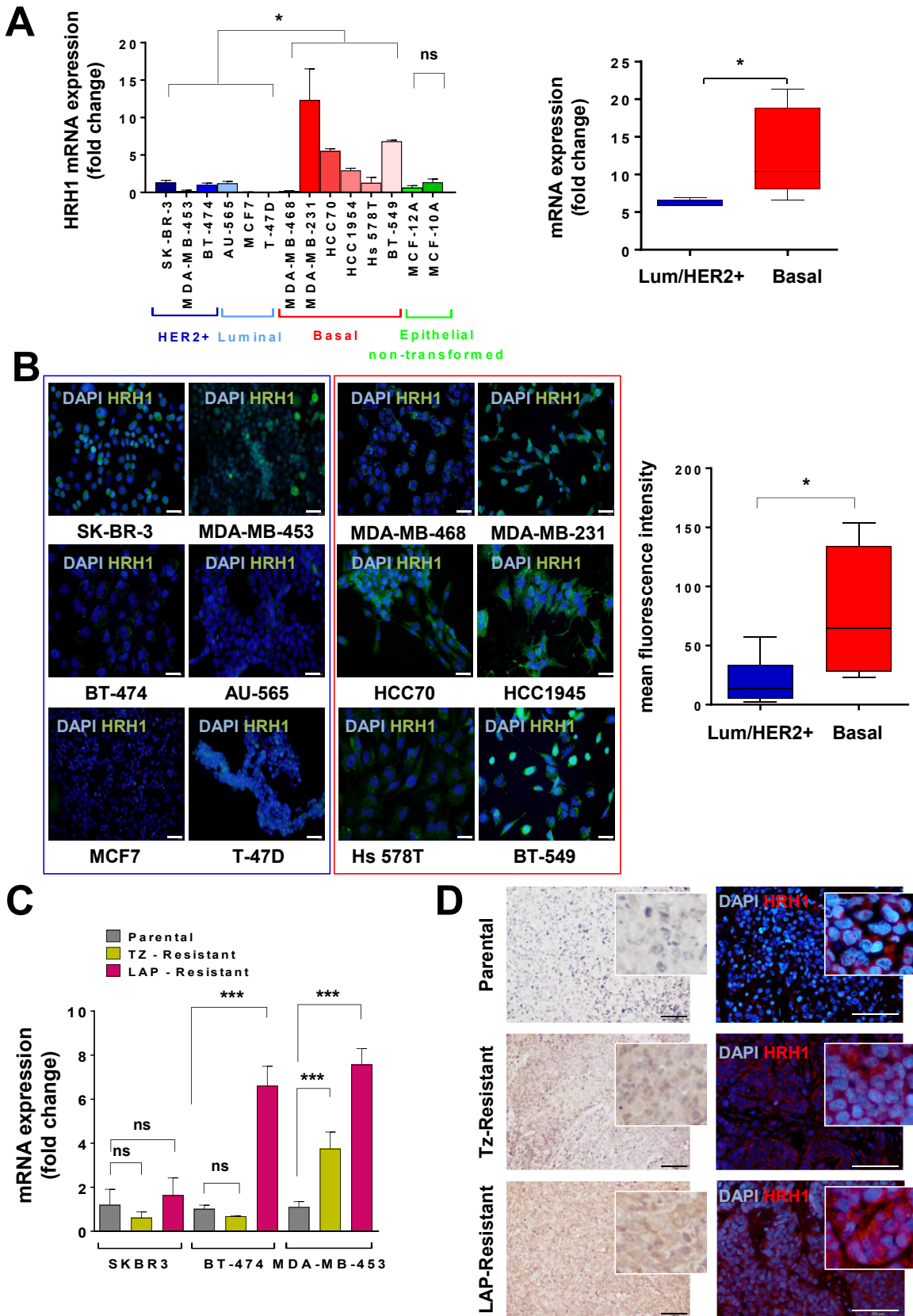


Fig. 1. Expression of HRH1 in BC cell lines.

(A) Quantitative real-time PCR (qPCR) was performed to determine the HRH1 mRNA levels in several human BC cell lines (left panel). The data were reported as fold changes of HRH1 mRNA expression in breast cancer cell lines relative to those of immortalized epithelial cell lines (MCF-10A and MCF-12A). Statistical analysis was performed using ordinary one-way ANOVA followed by Tukey's multicomparison test. * $p < 0,05$, ns: non-significant (left panel). Box plot of the samples shown in the left panel grouping luminal/HER2-enriched BC vs. basal BC cell lines (right panel). (mean \pm SEM; $n = 3$). Statistical analysis was performed using the Mann-Whitney test. * $p < 0,05$. (B) Representative

different times (70 min for short-time signaling pathway activation or 24 h for apoptosis-related experiments). The proteins were extracted using ice-cold radioimmunoprecipitation assay (RIPA) buffer supplemented with protease inhibitors (SIGMA; #S8820) and were quantified using the PIERCE method (Thermo Scientific; #23225). The proteins were separated by polyacrylamide gel electrophoresis and were transferred onto polyvinylidene difluoride (PVDF) membranes. The membranes were blocked in Tris-buffered saline, 0.1% Tween 20 (TBS/T) buffer containing 5% dry milk and were incubated overnight with primary antibodies at 4 °C: p38 mitogen-activated protein kinase alpha (p38 α) (Cell Signaling; #9212S), phospho-p38 mitogen-activated protein kinase (P-p38) (Cell Signaling; #9211S), protein kinase B (AKT) (Cell Signaling; #9272S), phospho-AKT (P-AKT) (Cell Signaling; #4060S), BAX (Cell Signaling; #5023S), Cleaved Caspase-3 (Cell Signaling; #9664S), ERK 1/2 (Cell Signaling; #9102S), phospho-ERK1/2 (P-ERK) (Cell Signaling; #9101S), p53 (Cell Signaling; #48818), phospho-p53 (SER15) (P-p53 (SER15)) (Cell Signaling; #9286), p21 (Cell Signaling; #2947), poly (ADP-ribose) polymerase (PARP) (BD Pharmingen; #51–66J9GR), glyceraldehyde-3-phosphate dehydrogenase (GAPDH) (Cell Signaling; #2118S), α -tubulin (Cell Signaling; #2144S), vimentin (Cell Signaling; #5741S). Membranes were then incubated with their respective secondary antibodies labeled with peroxidase for 1 h at RT and were visualized using an enhanced chemiluminescence system (ECL; GE Healthcare, UK; #RPN2209). Chemiluminescence was detected using the LAS-4000 image analyzer (FUJIFILM, Japan) and was quantified by densitometric analysis using Multi-Gauge software (FujiFilm Corporation, Japan).

qPCR

Total RNA was extracted from cells using an RNeasy mini kit (Qiagen, Germany; #74106) according to the manufacturer's protocol. One microgram of total RNA was used for reverse transcription using a High cDNA Reverse Transcription Kit (Applied Biosystems, CA, USA; #4368813). Quantitative real-time PCR was performed on a PCR machine using validated Taqman Gene Expression Assays (Applied Biosystems). Data analysis was based on the $\Delta\Delta C_t$ method with β -Actin as the housekeeping gene.

Immunohistochemistry

Paraffin-embedded 4 μ m tumor tissue sections were dewaxed in xylene and hydrated in an ethanol series. Antigens were retrieved with citrate buffer (pH 6), and samples were blocked with 1.5% normal goat serum (NGS) for 30 min at RT. Next, the tissues were incubated overnight at 4 °C with the primary antibody against P-ERK (Cell Signaling; #9101S) and HRH1 (Santa Cruz Biotechnology; sc20633). The samples were incubated with a rabbit anti-goat IgG biotinylated antibody (Amersham, UK; #111-065–003) for 1 h at RT followed by the ABC peroxidase system (Vector Laboratories, UK; #PK-6100), following the manufacturer's instructions. 3,3'-Diaminobenzidine (DAB, Sigma; #D4168) was used as a colorimetric substrate. The tissues were counterstained with hematoxylin (Sigma; #HHS80), and the slides were dehydrated in an ethanol series and were mounted with Cytoseal 60 (Sigma, #83104). The

samples were quantified using ImageJ software (NIH, MD, USA) considering the percentage of the P-ERK-positive area with respect to the total tumor area.

Cell cycle assay

To determine the effect of terfenadine on the cell cycle, BC cells were seeded in 6-well plates under sub-confluent conditions (10^6 /well) with complete media. After 24 h, the media were changed to serum-free media to synchronize the cells overnight. Each cell line was treated for 48 h with its IC50 terfenadine doses. Next, cells were detached and washed with PBS. Cells were fixed with 70% ethanol overnight at 4 °C and then were washed with PBS and resuspended in 200 μ l of PI/RNase staining buffer (BD Pharmingen, NJ, USA; #550825). The stained cells were analyzed by flow cytometry (Fortessa) and quantified using FACSDIVA software (BD Biosciences).

Incorporation of 5-bromo-2'-deoxyuridine (BrdU)

BC cells seeded in 6-well plates under sub-confluent conditions (10^6 /well) in complete media were synchronized using serum-free media overnight. The cells were then treated with terfenadine (MDA-MB-231 10,31 μ M; T-47D 5,81 μ M) for 48 h. BrdU (10 μ M/well) was added and left to incorporate into the newly synthesized DNA of replicating cells for 3 h. The cells were harvested in PBS and fixed with 70% ethanol overnight. The cells were then permeabilized and denaturalized with 2 M HCl and 0.5% Triton X-100 for 1 h at RT. Next, 0,1 M Na₂B₄O₇ was used to neutralize HCl for 20 min at RT. Anti BrdU-FITC antibody (1:20; DAKO, Denmark; #F7210) was added and kept in the dark for 1 h after PBS washing. After incubation with RNase (0.4 mg/ml) and PI (12,5 μ g/ml) for 20 min at RT in the dark, the samples were analyzed using FACS.

3-(4,5-Dimethylthiazol-2-yl)-2,5-diphenyltetrazolium bromide (MTT) assay

The Cell Titer 96 Aqueous One Solution Cell Proliferation Assay Kit (Promega, #G3581) was used to assess the possible effect of terfenadine, cimetidine (Sigma, #C4522) or thioperamide maleate (Sigma, #T123) on BC cell line proliferation. Briefly, sub-confluent cultures of BC cell lines were incubated for 72 h in the presence of increasing concentrations of terfenadine (0–25 μ M), cimetidine (0,1–100 μ M), thioperamide maleate (0,1–100 μ M), trastuzumab (0–250 μ g/ μ l) or lapatinib (0–6,25 μ M) in 96-well plates in sextuplicate. For color development, 20 μ l of tetrazolium MTT was added to each well and, after incubation for 30–45 min at 37 °C, the plate was read on a microplate spectrophotometer (Molecular Dynamics) at 490 nm (test wavelength) and 690 nm (reference wavelength). IC50, curve fitting and statistical analysis was performed according to the extra sum of squares F-test principle using Graph Pad Prims[®] Software. P values < 0,05 were considered statistically significant.

Wound-healing assay

The cells were seeded in 6-well plates and were cultured to 80–90% of confluence. Confluent monolayers were scratched using

immunofluorescence images of HRH1 staining. Magnification, 20 \times . DAPI was used as a counterstain for nuclei. Luminal and HER2-enriched BC cells were gated in a blue square, and basal BC cells were gated in a red square (left panels). Box plot of the mean fluorescence intensity of the samples shown in Fig. 1B (left panels) grouping luminal/HER2-enriched BC vs. basal BC cell lines. Statistical analysis was performed using the Mann-Whitney test. *p < 0,05 (C) Quantitative real-time PCR (qPCR) was performed to determine the HRH1 mRNA levels in parental and -HER2 targeted therapies resistant SK-BR-3, BT-474, and MDA-MB-453 cells lines. Statistical analysis was performed using ordinary one-way ANOVA followed by Tukey's multicomparison test. ns: non-significant, ***p < 0,001. (D) Representative HRH1 staining in the MDA-MB-453 parental, trastuzumab (TZ)- and lapatinib (Lap)-resistant tumors by immunohistochemistry (left column) and immunofluorescence (right column). Scale bar, 50 μ m. (For interpretation of the references to color in this figure legend, the reader is referred to the Web version of this article.)

a plastic pipette tip to draw a linear wound. The media were then replaced with media containing terfenadine (IC50 dose for each cell line), and the cells were incubated at 37 °C for 24 h. Images were captured at the indicated time points using a LEICA DFC295/DMIL LED microscope and ZEISS AXIOVERT200 at 4X magnification from five randomly selected fields in each sample. The distance between the opposing edges of the wound was measured in micrometers by ImageJ software (NIH, MD, USA).

Murine experiments

All *in vivo* experiments were approved by the Hospital Clinic of Barcelona (HCB) ethics committee according to the guidelines established by the Catalonian government in accordance with the principles of the Helsinki Declaration.

Five-week-old female athymic nude Foxn 1nu nu/nu mice (athymic nude) were obtained from Janvier and were kept at the HCB Medical School Animal Laboratory under pathogen-free conditions at constant ambient temperature (22–24 °C) and humidity (30–50%). After each experiment, the mice were anesthetized and euthanized in accordance with institutional guidelines.

Terfenadine efficacy study in basal and luminal BC cell lines

MDA-MB-231 and T-47D BC cells (2.5×10^5 and 2×10^6 cells, respectively) were injected orthotopically into two mammary fat pads of each animal. Cells were injected as a mixture (1:1 ratio) of PBS:Matrigel (BD Bioscience, #10429212) at a total volume of 150 μ l.

Tumor growth was measured twice weekly with a digital caliper, and the tumor volume was calculated as $V = (D \cdot d^2)/2$. When the tumor volume reached 100 mm³, the mice were randomized to two groups (control and experimental (terfenadine treated)). The experimental group was treated daily intraperitoneally with 10 mg/kg of terfenadine for four weeks as previously described [29]. A saline solution was administered to the control group. Once treatment was finished, mice were sacrificed, and tumors were surgically recovered, measured, fixed in 4% PFA (PanReac), and embedded in paraffin for further immunohistochemistry analysis.

Role of HRH1 inhibition in BC cells resistant to HER2-targeted therapies

Xenograft tumors were established by orthotopic injection into two mammary fat pads per mice at a mixture (1:1 ratio) of 1.5×10^6 MDA-MB-453 BC cells (parental and trastuzumab- and lapatinib-resistant) in PBS:Matrigel (total volume: 150 μ l). Tumor growth was measured as explained above. Once the tumors reached volumes of 100 mm³, the mice were randomized to two groups, and treated with terfenadine or vehicle for four weeks as previously described [29]. Changes in the tumor volume between groups were analyzed by ANOVA. P-values < 0,05 were considered statistically significant.

Statistical analysis

Comparisons between two groups were performed using the Mann-Whitney *t*-test (two-tailed). Comparison between more than 2 groups was performed by ordinary one-way ANOVA followed by Tukey's multicomparison test (Graph Pad Prims[®] Software). For all tests, $p < 0,05$ was considered statistically significant.

Results

HRH1 is overexpressed in basal and HER2-targeted therapy-resistant BC cells

Recently, using bioinformatic tools to interrogate various published BC databases, we found that HRH1 was overexpressed in basal and HER2-enriched BC samples [14]. Analysis of HRH1 expression using the GOBO database showed that it was significantly correlated with shorter overall survival ($p < 0,0001$) and with distant metastasis-free survival ($p < 0,0001$) [14]. These results led us to study the role of HRH1 in BC progression. We first characterized HRH1 expression, at the mRNA and protein levels in a wide panel of BC cell lines classified according to their molecular profile (resembling the different BC subtypes) [30] (Fig. 1A–B). Most basal BC cell lines express higher levels of HRH1 than luminal and HER2-enriched BC cell lines and normal mammary epithelial cell lines (Fig. 1A). Analysis of HRH1 protein expression by immunofluorescence corroborated the mRNA results, showing that HRH1 is overexpressed at the protein level in basal BC cell lines (Fig. 1B and Supplementary Fig. S1A). Two HER2-enriched cell lines (MDA-MB-453 and BT-474) expressed very low levels of HRH1, while the other (SK-BR-3) expressed moderate levels (Fig. 1B and Supplementary Fig. S1A).

Conversely, there was no difference in the expression of the other members of the histamine receptor family (HRH2 and histamine receptor 3 (HRH3)) when comparing luminal and basal BC cell lines (Supplementary Fig. S1B). Histidine decarboxylase (HDC) is the only enzyme that catalyzes the decarboxylation of histidine to form histamine (HRH1-4 ligand). Analysis of its mRNA expression in our panel of BC cell lines and normal mammary epithelial cells showed no significant differences (Supplementary Fig. S1B). Histamine receptor 4 (HRH4) was not detected in BC or normal mammary epithelial cells (data not shown).

We further analyzed the expression of HRH1, HRH2 and HRH3 in a panel of trastuzumab- and lapatinib-resistant HER2-enriched cell lines (Fig. 1C and Supplementary Fig. S1C). BT-474 and MDA-MB-453 lapatinib-resistant cell lines showed a significant increase in HRH1 expression compared with parental cells at the mRNA level. In addition, in MDA-MB-453 trastuzumab-resistant cell lines, the HRH1 mRNA levels were significantly higher than those in parental cells (Fig. 1C). HRH2 was significantly overexpressed in BT-474 and MDA-MB-453 lapatinib-resistant cells, and HRH3 up-regulation was observed only in BT-474 lapatinib-resistant cells. Finally, HDC was significantly overexpressed in lapatinib-resistant cells (Supplementary Fig. S1C). Together, those results suggest the possible implication of enhanced histamine-HRH1 signaling in the resistant phenotype to lapatinib and trastuzumab in HER2-enriched BC.

To test whether up-regulation of HRH1 was maintained in resistant tumors *in vivo*, we inoculated MDA-MB-453 parental and trastuzumab- and lapatinib-resistant cells orthotopically in the mammary fat pad of athymic nude mice. After 1 month, the tumors were extracted, and HRH1 expression was tested by immunohistochemistry and immunofluorescence (Fig. 1D). Our results showed that trastuzumab- and lapatinib-resistant tumors overexpressed HRH1 (Fig. 1D).

All together, these results suggested that HRH1 signaling is up-regulated in basal BC and HER2-targeted therapy-resistant cell lines.

Inhibition of HRH1 activity in basal BC cells leads to sub-G0 accumulation and suppresses proliferation

Because histamine has been shown to positively influence

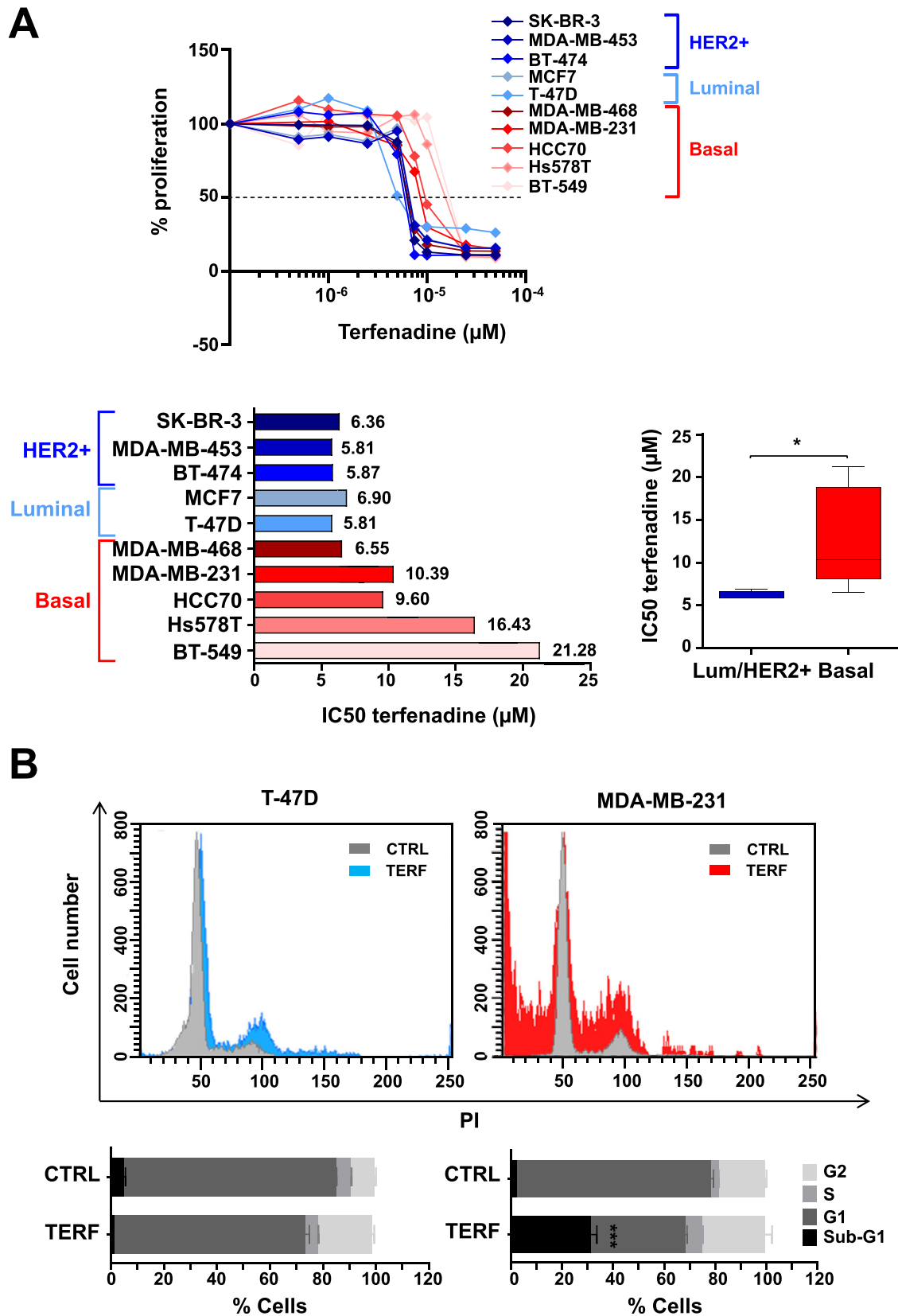


Fig. 2. Terfenadine effects on cell viability and cell proliferation in BC cell lines.

(A) Cell viability was evaluated in a wide panel of BC cell lines by the MTT assay after treating cells for 48 h with increasing doses of terfenadine (1–100 μM) (upper panel). Bar charts of IC50 values obtained using the cell survival MTT assay depicted in Fig. 2A (upper panel). The IC50 value for each cell line was reported. Statistical analysis was performed using the Mann-Whitney test. *** $p < 0,001$ (lower left panel). Box plot of the terfenadine IC50 (μM) values calculated from the MTT assay curves (Fig. 2A, upper panel) grouping luminal/HER2-enriched BC vs. basal BC cell lines. Statistical analysis was performed using the Mann-Whitney test. * $p < 0,05$. (B) Cell cycle profiles of T-47D (luminal) BC cells and MDA-MB-231 (basal) BC cells grown under either normal culture conditions (gray curve) or treated with 10 μM terfenadine (red and blue curves, MDA-MB-231 and T-47D respectively) for 48 h (upper panel). Graphic representation of the cell cycle distribution in percentages for the populations evaluated (lower panel). Statistical analysis was performed using the Mann-Whitney test. *** $p < 0,001$. (For interpretation of the references to color in this figure legend, the reader is referred to the Web version of this article.)

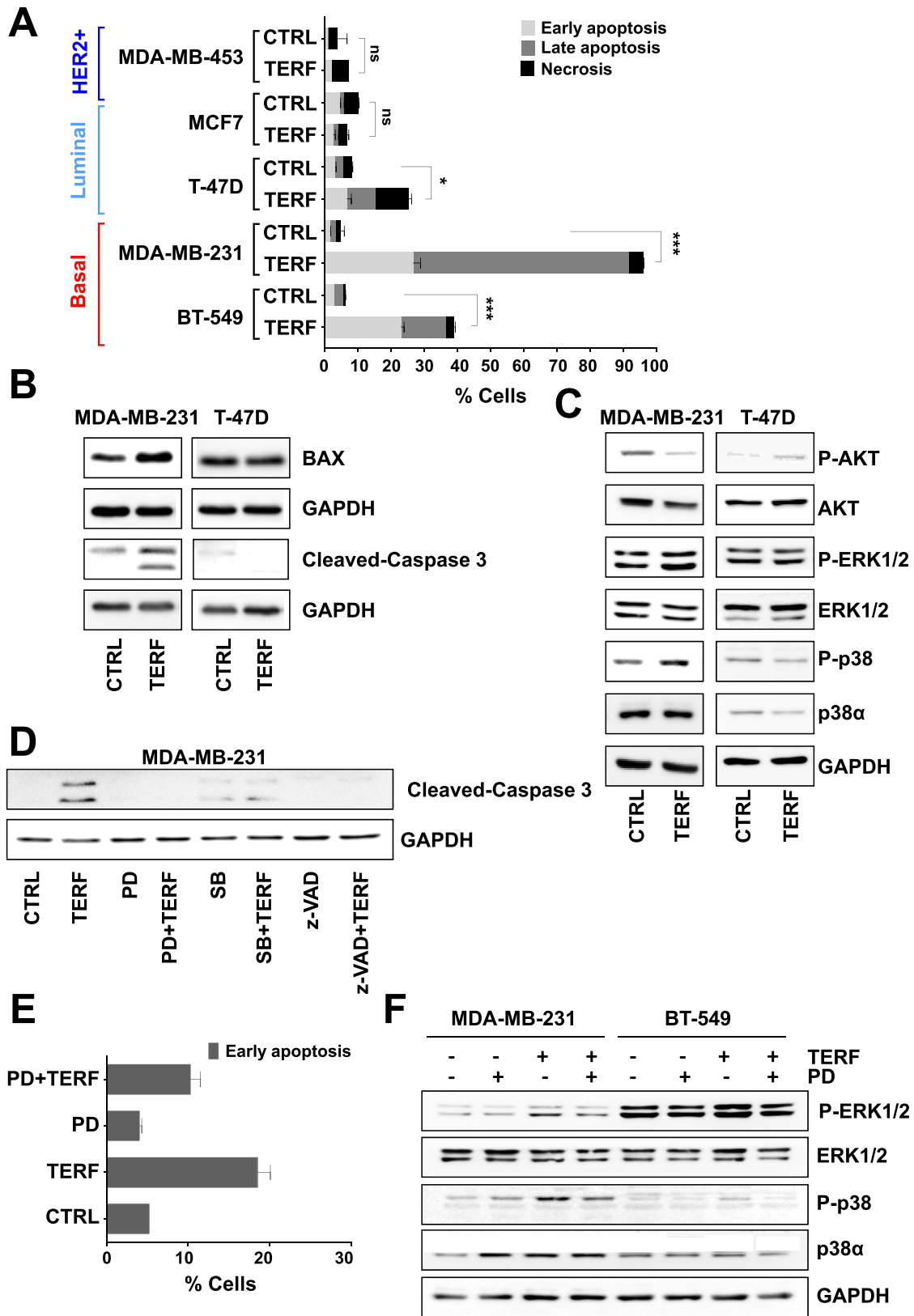


Fig. 3. Terfenadine effects on cell apoptosis in BC cell lines.

(A) HER2-enriched (MDA-MB-453), luminal (MCF7 and T-47D) and basal (MDA-MB-231 and BT-549) BC cell apoptosis at different stages (early, late and necrosis) was determined after terfenadine treatment with doses according to the IC50 values of each cell line (reported in Fig. 2A, left lower panel) or vehicle (ethanol) by the Annexin V method and measured by flow cytometry. n = 3. Statistical analysis was performed using the Mann-Whitney test. *p < 0,05, ***p < 0,001 ns: non-significant. (B) Bax and cleaved Caspase 3 proteins were determined by western blot analysis after 24 h of treatment with terfenadine with doses according to the IC50 values (reported in Fig. 2A, left lower panel) for MDA-MB-231 and T-47D cells. GAPDH served as the internal control. (C) Phosphorylation of AKT, ERK and p38 were determined by western blotting using antibodies specific for the

tumor growth [31], and our results showed that its receptor (HRH1) is overexpressed in basal and HER2-targeted therapy-resistant BC cells, we next examined the effect of blocking histamine receptors activity on the proliferation of BC cell lines (Fig. 2A and Supplementary Fig. S2A) using selective chemical histamine receptor antagonists: terfenadine (a specific HRH1 inhibitor), cimetidine (a specific HRH2 inhibitor) and thioperamide (an HRH3-HRH4 inhibitor). We first determined the cytotoxic effect of these inhibitors on cell survival. Cells were incubated with the above-mentioned inhibitors at increasing concentrations for 72 h. Terfenadine treatment showed dose-dependent effects on cell proliferation in all BC cell lines (Fig. 2A, upper panel). Cimetidine and thioperamide showed no suppressive activity on cell proliferation (Supplementary Fig. S2A). However, comparing IC50 values, terfenadine suppression of luminal/HER2-enriched BC cell proliferation was more effective than that of basal BC cell proliferation (Fig. 2A, lower panels) because higher doses were needed to reach IC50 in basal BC cells.

To further assess the anti-proliferative effects of terfenadine, we performed 5'BrdU incorporation analysis and found that treatment with terfenadine (MDA-MB-231 10,39 μ M; T-47D 5,81 μ M) for 48 h decreased proliferation in both basal and luminal cell lines (Supplementary Fig. S2B). We also analyzed the effect of histamine on BC cell proliferation and found induction of proliferation in basal and luminal cell lines (Supplementary Fig. S2C).

Although T-47D and MCF7 luminal cells express low levels of HRH1 (Fig. 1A–B), they express high levels of HRH2 and HRH3 (Supplementary Fig. S1B); therefore, the effect of histamine on these cells might be mediated by HRH2 and/or HRH3 pathways.

Next, we analyzed the effect of terfenadine on BC cell death: we evaluated the BC cell cycle pattern after terfenadine treatment for 48 h and found the accumulation of MDA-MB-231 basal BC cells in the sub-G0 phase of the cell cycle (Fig. 2B, right). Meanwhile, the luminal cell cycle profile was not affected by terfenadine (Fig. 2B, left). This suggested that HRH1 signaling is directly involved in basal BC proliferation by driving progression of cancer cells from the G1 to S phase and that inhibition of the receptor leads to accumulation in the sub-G1 phase of the cell cycle, indicative of DNA fragmentation, probably due to apoptosis.

Inhibition of HRH1 induces apoptosis in basal BC cells

We have previously shown that terfenadine led to an accumulation in the sub-G1 phase of the basal BC cell cycle (Fig. 2B), suggesting apoptosis as a possible mechanism of cell death. The apoptotic effect of terfenadine in basal BC cells was confirmed by the annexin V-FITC/PI staining assay. Treatment with terfenadine for 48 h induced apoptosis in MDA-MB-231 and BT-549 cells (Fig. 3A), while MCF7 luminal cells, and MDA-MB-453, HER2-enriched cells, were resistant to the induction of apoptosis by terfenadine (Fig. 3A). Terfenadine prompted apoptosis in T-47D luminal cells as well, even if its effect was much smaller than that in basal BC cell lines.

Western blot analysis of apoptosis markers showed that terfenadine increased BAX and cleaved-caspase 3 in MDA-MB-231

(basal) but not T-47D (luminal) cell lines (Fig. 3B), suggesting that the inhibition of HRH1 induces apoptosis in basal cell lines through the apoptotic mitochondrial pathway. Interestingly, treatment with terfenadine also induce p53 phosphorylation in MDA-MB-231 cells but not in T-47D cells (Supplementary Fig. S2D) suggesting that terfenadine effects might be mediated via p53 activation.

We also analyzed the stress-signaling pathways involved in proliferation and survival. Our results showed that the inhibition of HRH1 inhibits AKT activation while promoting ERK and p38 α activation in MDA-MB-231 basal BC cells (Fig. 3C), and these pathways remained undisturbed in T-47D luminal cells (Fig. 3C). Moreover, activation of caspase 3 by terfenadine in the MDA-MB-231 basal cells was reversed when the cells were treated in the presence of either a MEK1 inhibitor (PD98059), p38 α/β inhibitor (SB203580) or caspase inhibitor (z-VAD) (Fig. 3D). Furthermore, the apoptotic effect of terfenadine was partially abolished when MDA-MB-231 (basal) BC cells were pre-treated for 24 h with PD98059 (Fig. 3E), which also inhibited ERK1/2 and p38 α/β activation (Fig. 3F) in basal cell lines (MDA-MB-231 and BT-549). These results suggested that HRH1 inhibition in basal cells induces apoptosis through MAPKs, BAX and caspase 3 activation.

HRH1 expression in BC cells promotes cell motility

The effects of the targeted inhibition of HRH1 on cell migration were examined by the wound-healing assay (Fig. 4A–B). When confluent monolayers of cells were treated with terfenadine, basal BC cell lines MDA-MB-231 and BT-549 exhibited slower migration speeds than controls (in which the gap was rapidly closed) (Fig. 4A). Time course results revealed that the wound width was significantly larger at both earlier (6 h for MDA-MB-231; 12 h for BT-549) and later (12 h for MDA-MB-231; 24 h for BT-549) time points in cells treated with terfenadine compared with non-treated cells (Fig. 4A). Luminal (MCF7, T-47D) and HER2-enriched cell lines (MDA-MB-453) showed limited migratory potential in controls (non-treated cells), and HRH1 inhibition showed no effect on cell motility (Fig. 4B). To further identify the role of terfenadine on the migration capability of basal and luminal cell lines, we analyzed the expression of epithelial mesenchymal transition (EMT) markers in BT-549 and MDA-MB-231 (basal) cells, T-47D (luminal) cells and MDA-MB-453 (HER2-enriched) BC cell lines treated with terfenadine. EMT can be initiated by the overexpression of certain proteins—among them, snail family zinc finger 2 (SLUG), twist family bHLH transcription factor 1 (TWIST), and vimentin—in cells that have been observed in the progression from the *in situ* to invasive forms of BC [32]. We found that basal cell lines express high levels of TWIST and SLUG than luminal and HER2-enriched cell lines (Fig. 4C). However, treatment with terfenadine had no effect on TWIST or SLUG expression in BT-549 (basal) cells (Fig. 4D). Nevertheless, the protein levels of vimentin were markedly decreased (45%) in basal cells when treated with terfenadine (Fig. 4E). Taken together, these results suggested that terfenadine might prevent basal BC cell motility by inhibiting the expression of the mesenchymal marker vimentin.

phosphorylated, activated forms of AKT (p-AKT), ERK (p-ERK 1/2) and p38 (p-p38) in MDA-MB-231 and T-47D cells after 70 min of treatment with terfenadine 5 μ M of MDA-MB-231 and T-47D cells. The membranes were stripped and reprobed with antibodies against total AKT, ERK 1/2 and p38 α . GAPDH served as the internal control. (D) MDA-MB-231 cells were pre-treated overnight (O/N) with a MEK1 inhibitor (PD98059) (lines 3–4), a p38 α/β inhibitor (SB203580) (lines 5–6) or a caspase inhibitor (z-VAD) (lines 7–8) followed or not by treatment with terfenadine 5 μ M for 24 h. Lane 2, as a positive control, was treated with terfenadine alone during 24 h. The protein levels were analyzed by western blotting. GAPDH served as the internal control. (E) Graphic representation of the percentage of early apoptotic cells as determined by Annexin V analysis by flow cytometry in MDA-MB-231 cells grown under either normal culture conditions (control) or treated with terfenadine 5 μ M and MEK1 inhibitor (PD98059) 40 μ M alone or in combination for 48 h (F) MDA-MB-231 and BT-549 (two basal BC cell lines) were pre-treated O/N with a MEK1 inhibitor (PD98059) (lanes 2, 4, 6, 8) followed (lanes 4, 8) or not (lanes 2, 6) by treatment with terfenadine 5 μ M for 24 h. Lanes 3 and 7 were treated with terfenadine alone during 70 min. Phospho ERK (p-ERK1/2), total ERK1/2, phospho p38 (p-p38) and total p38 α protein levels were analyzed by western blotting. GAPDH served as the internal control.

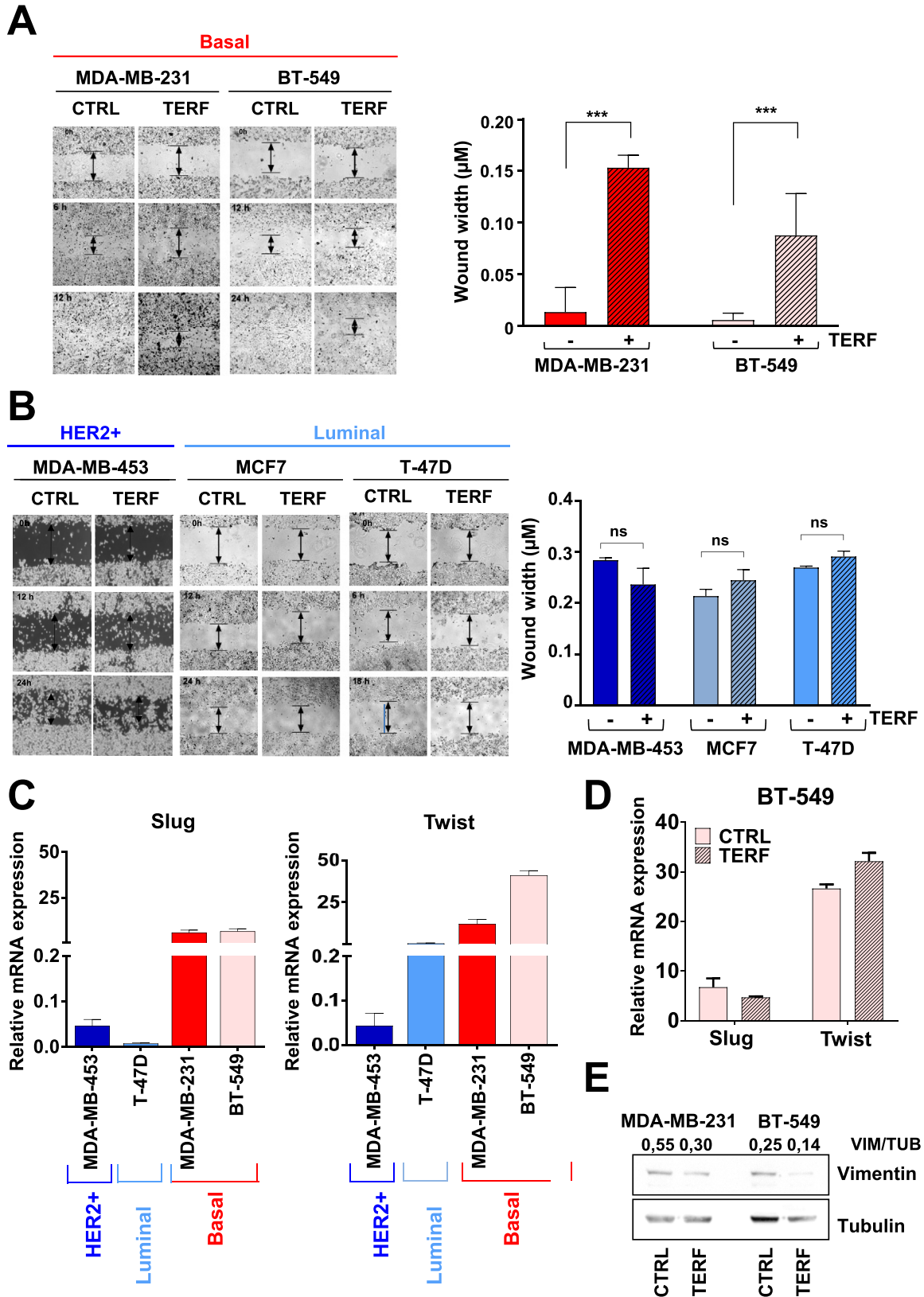


Fig. 4. Terfenadine effects on cell motility in BC cell lines.

(A) Image-based monitoring was performed at 6 h and 12 h for MDA-MB-231 and 12 h and 24 h for BT-549 using phase contrast and $4\times$ magnification. Kinetic images shown for untreated (control) or treated cells with terfenadine with doses according to the IC₅₀ values (reported in Fig. 2A, left lower panel) (left panel). Quantification of the wound width (μm) at the end time point is shown in the right panel. Statistical analysis was performed using the Mann-Whitney test. *** $p < 0,001$. (B) Image-based monitoring of MDA-MB-453 (HER2-enriched), MCF7 and T-47D (luminal) BC cell migration. Imaging was performed over 24 h (MDA-MB-453 and MCF7) and 18 h (T-47D) using inverted microscopy (MDA-MB-453) and phase contrast microscopy (MCF7 and T-47D) at $4\times$ magnification. Kinetic images shown for untreated (control) or treated cells with terfenadine according to the IC₅₀ values for each cell line (reported in Fig. 2A, left lower panel) (left panel). Quantification of the wound width (μm) at the end time point is shown in the right panel. Statistical analysis was performed using the Mann-Whitney test. ns: non-significant. (C) Quantitative real-time PCR (qPCR) was performed to determine the SLUG and TWIST mRNA levels in HER2-enriched (MDA-MB-453), luminal (T-47D) and basal (MDA-MB-231 and BT549) BC cell lines. (D) Quantitative real-time PCR (qPCR) was performed to determine the SLUG and TWIST mRNA levels in BT-549 BC cell lines after treatment with terfenadine 21,28 μM for 48 h. (E) Vimentin protein expression was determined by western blot analysis after 48 h of treatment with terfenadine (MDA-MB-231 10,39 μM ; BT-549 21,28 μM). GAPDH served as the internal control. Representative western blot bands and quantification analysis are reported.

Inhibition of HRH1 reduces tumor progression in vivo

To further evaluate whether HRH1 inhibition can prevent basal tumor cell growth *in vivo*, we injected basal MDA-MB-231 and luminal T-47D cells orthotopically into athymic nude mice. Once the tumors reached 100 mm³, we administered terfenadine 10 mg/kg intra-peritoneally (i.p.) once a day for 4 weeks (Fig. 5A). Terfenadine slightly reduced basal MDA-MB-231-derived tumor growth, although the differences did not reach statistical significance (Fig. 5B–C). T-47D luminal cell tumor growth was unaffected (Fig. 5D), suggesting that only basal BC cells might depend on HRH1 for proliferation and survival *in vivo*.

Because our *in vitro* results indicated that HRH1 inhibition promotes ERK1/2 and p38 α / β phosphorylation, we stained the tumors to detect phospho-ERK and phospho-p38 α . Tumors from animals treated with terfenadine showed higher levels of phospho-ERK than tumors from untreated animals (Fig. 5E). No variation in phospho-p38 α expression was detected between the two groups of mice (data not shown). These results suggest that HRH1 might prevent basal tumor cell growth by inducing apoptosis through ERK activation, further demonstrating the important role of HRH1 in the development and progression of basal-subtype breast tumors.

Inhibition of HRH1 induces apoptosis in HER2-targeted therapy-resistant cell lines

We have previously seen that HRH1 expression was increased significantly in patients with HER2-enriched BC [14]. Furthermore, we found that trastuzumab- and lapatinib-resistant cell lines overexpressed HRH1 (Fig. 1C–D). To test whether HRH1 and histamine can mediate survival in these cells, we performed viability assays treating parental and resistant cells with trastuzumab or lapatinib in the presence of histamine. We found that, while histamine did not affect the sensitivity of parental cells to trastuzumab or lapatinib, it increased the viability of trastuzumab- and lapatinib-resistant cells (Fig. 6A). These results suggested that resistant cells might benefit from histamine-HRH1 signaling for survival.

We next tested whether terfenadine could induce cell death in resistant cells. As expected, trastuzumab- and lapatinib-resistant cells were more sensitive to terfenadine than parental cells; therefore, they have lower IC50s (Fig. 6B). Next, we analyzed the cell cycle pattern of lapatinib- and trastuzumab-resistant cells after treatment with terfenadine for 48 h and found an accumulation of trastuzumab-resistant BC cells in the sub-G0 phase of the cell cycle (Fig. 6C). However, the lapatinib-resistant cells cell cycle profile was not affected by terfenadine treatment (Fig. 6C). These data suggested that HRH1 signaling is directly involved in HER2-enriched trastuzumab-resistant BC cell proliferation by driving the progression of cancer cells from G1 to S phase, and inhibition of the receptor leads to accumulation in the sub-G0 phase of the cell cycle.

Finally, we tested whether treatment with terfenadine inhibited the growth of trastuzumab-resistant cell lines *in vivo*. We inoculated parental and trastuzumab-resistant cells orthotopically into athymic nude mice and allowed them to grow until the tumors reached 100 mm³. We then treated the animals with terfenadine 10 mg/kg i.p. once a day for 4 weeks. The results showed that, while terfenadine does not affect MDA-MB-453 parental cell growth *in vivo*, it inhibits the growth of MDA-MB-453 trastuzumab-resistant cells (Fig. 6D), suggesting that HRH1 inhibition might sensitize HER2-targeted therapy-resistant cells to apoptosis.

Discussion

Our discovery that HRH1 is differentially overexpressed in basal

and HER2-enriched breast tumor samples revealed new features of histamine signaling and new perspectives in the pharmacology of HRH1 [14]. In the present study, a wide panel of BC cell lines previously classified according to their molecular profile (resembling the different BC subtypes) was used to strengthen the previous observations using a bioinformatics approach and several BC databases and to further study the role of HRH1 in basal and HER2-targeted therapy-resistant BC biology. We have evidenced that most basal BC cell lines express higher levels of HRH1 than luminal BC cell lines and normal mammary epithelial cell lines, in accordance with what we have previously seen in patients [14]. Moreover, up-regulation of HRH1 was also maintained in HER2-targeted therapy-resistant tumors *in vivo*. To investigate functional characteristics of HRH1, a specific HRH1 inhibitor, terfenadine, was employed *in vitro* and *in vivo* to better understand the role of HRH1 in basal and HER2-targeted therapy-resistant BC cells. Remarkably, HRH1 blockade led to a reduction in proliferation and increased apoptosis only in basal and HER2-targeted therapy-resistant BC cells, suggesting that, in these cells, HRH1 signaling is directly involved in proliferation by driving the progression of cancer cells from the G1 to S phase and preserving cells from apoptosis. These results are in agreement with the significant growth inhibition of several human cancer cells, through the induction of G0/G1 cell-cycle arrest and apoptosis, induced by terfenadine [33]. In addition, in melanoma cells, apoptosis and autophagy through ROS-dependent and -independent mechanisms are prompted by terfenadine [28]. Furthermore, specific CYP2J2 inhibitors, related to terfenadine, markedly attenuated the neoplastic phenotypes of several carcinoma cells [34]. However, some studies have also shown that terfenadine may induce anti-proliferative and apoptotic activity in melanoma cells and human hormone-refractory prostate cancer independently of HRH1 [35–37]. Nevertheless, we found that terfenadine induced two apoptotic markers, BAX and cleaved-caspase 3 up-regulation, as well as p53 activation, only in the basal phenotype, suggesting that HRH1 inhibition induces apoptosis in basal cell lines through the apoptotic mitochondrial pathway. It has been reported that terfenadine-treated thymocytes undergo a reduction in mitochondrial membrane potential and release of cytochrome C from the mitochondria to the cytosol [38]. To determine the molecular mechanisms underlying the antitumor activity of terfenadine, its effects on cell proliferation and apoptosis signaling pathways were assessed. It is widely reported that AKT and the MAPK signaling pathways regulate proliferation and apoptosis [39,40]. Modulations in p38 MAPK are frequently linked to apoptosis [41,42], and the ERK pathway has been associated with cell survival [40]. For these reasons, we analyzed the activation of some pivotal proteins of these signaling pathways (such as pAKT, pp38 and pERK 1/2) in basal and luminal cell lines. As expected, terfenadine inhibited the activation of AKT and increased phospho-p38 MAPK levels in basal BC cells. In addition, terfenadine in basal cell lines, despite prompting apoptosis, also fostered the phosphorylation of ERK1/2 pointing towards a pro-apoptotic role of ERK1/2 in these BC cells. Moreover, caspase 3 activation by terfenadine in basal cells was reversed when the cells were treated in the presence of either a MEK1 inhibitor (PD98059), a p38 α / β inhibitor (SB203580), or a caspase inhibitor (z-VAD). Finally, given that the apoptotic effect of terfenadine was partially abolished when BC cells were pre-treated with PD98059, we speculate that, in these cell lines, in response to aberrant signaling (HRH1 blockade), tumor suppressor mechanisms may be activated, inducing growth inhibition and apoptosis. Indeed, it has been shown that, in some cases, ERK activation could increase the apoptotic action of pro-apoptotic proteins [43]. Moreover, the removal of soluble factors from primary cultures of murine renal proximal tubular cells leads to ERK1/2 activation-induced

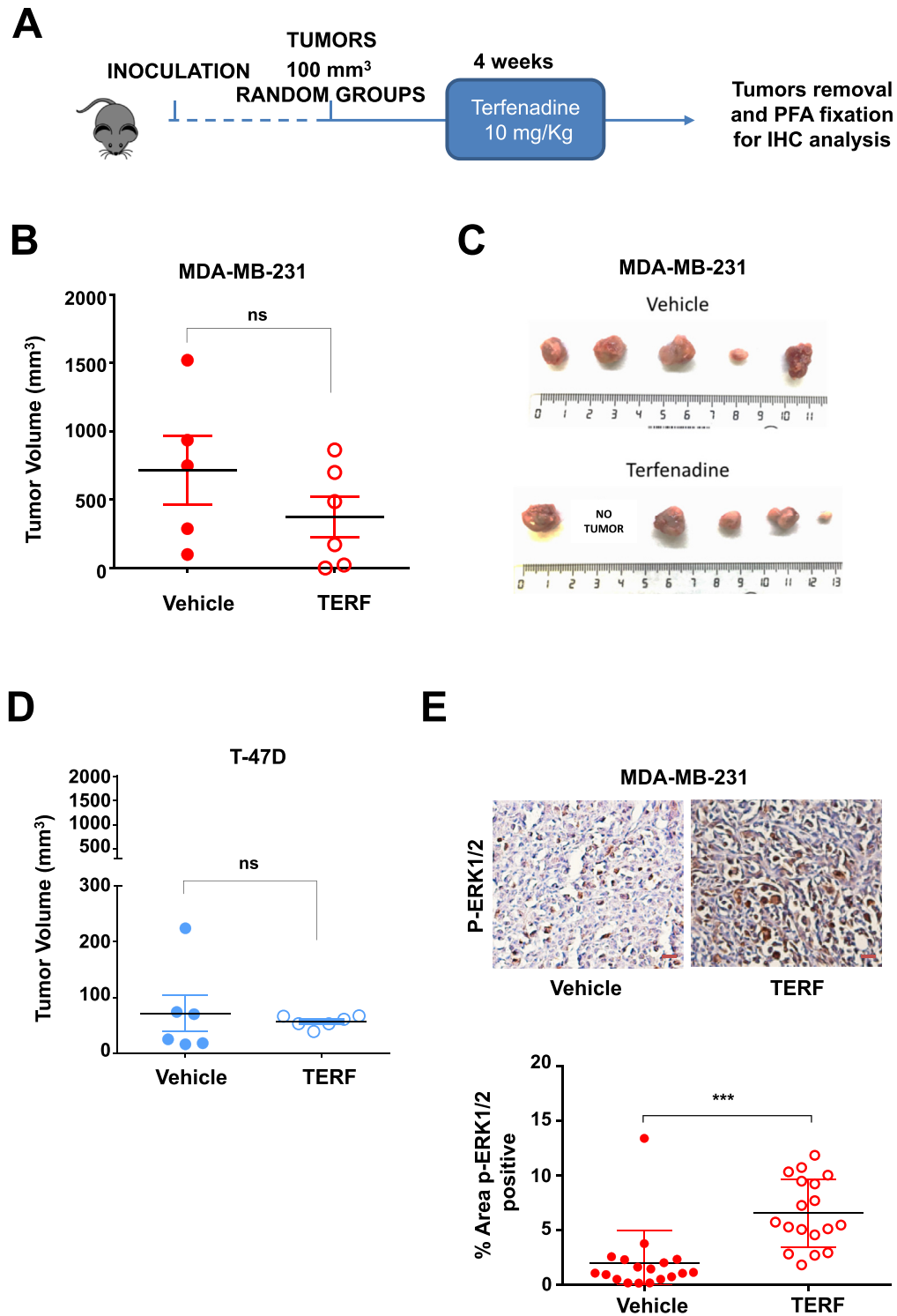


Fig. 5. *In vivo* model and effects of HRH1 inhibition on BC cell xenograft evolution.

(A) Timeline of the *in vivo* protocol applied. Briefly, MDA-MB-231 and T-47D BC cells were injected orthotopically into two mammary fat pads of each animal. When the tumor volume reached 100 mm³ (tumor volume: $V = (D \cdot d^2)/2$), the mice were randomized into two groups (control and experimental (terfenadine treated)). The experimental group was treated daily intraperitoneally with 10 mg/kg of terfenadine for four weeks. A saline solution was administered to the control group. Next, the mice were sacrificed, and their tumors were surgically recovered, measured, fixed in 4% paraformaldehyde (PFA), and embedded in paraffin for further immunohistochemistry analysis. (B,D) Tumor growth for MDA-MB-231 (B) and T-47D (D) $n = 6$. Statistical analysis was performed using the Mann-Whitney test. ns: non-significant (C) Surgically removed MDA-MB-231 tumor tissues from nude mice 28 days post-randomization. (E) Immunohistochemical staining (upper panel) and quantification (lower panel) in MDA-MB-231 tumor tissue of the mice treated with vehicle (upper panel, left) or terfenadine (upper panel, right) was used to detect phospho-ERK (p-ERK1/2) protein; scale bars, 50 μ m. Statistical analysis was performed using the Mann-Whitney test. *** $p < 0,001$.

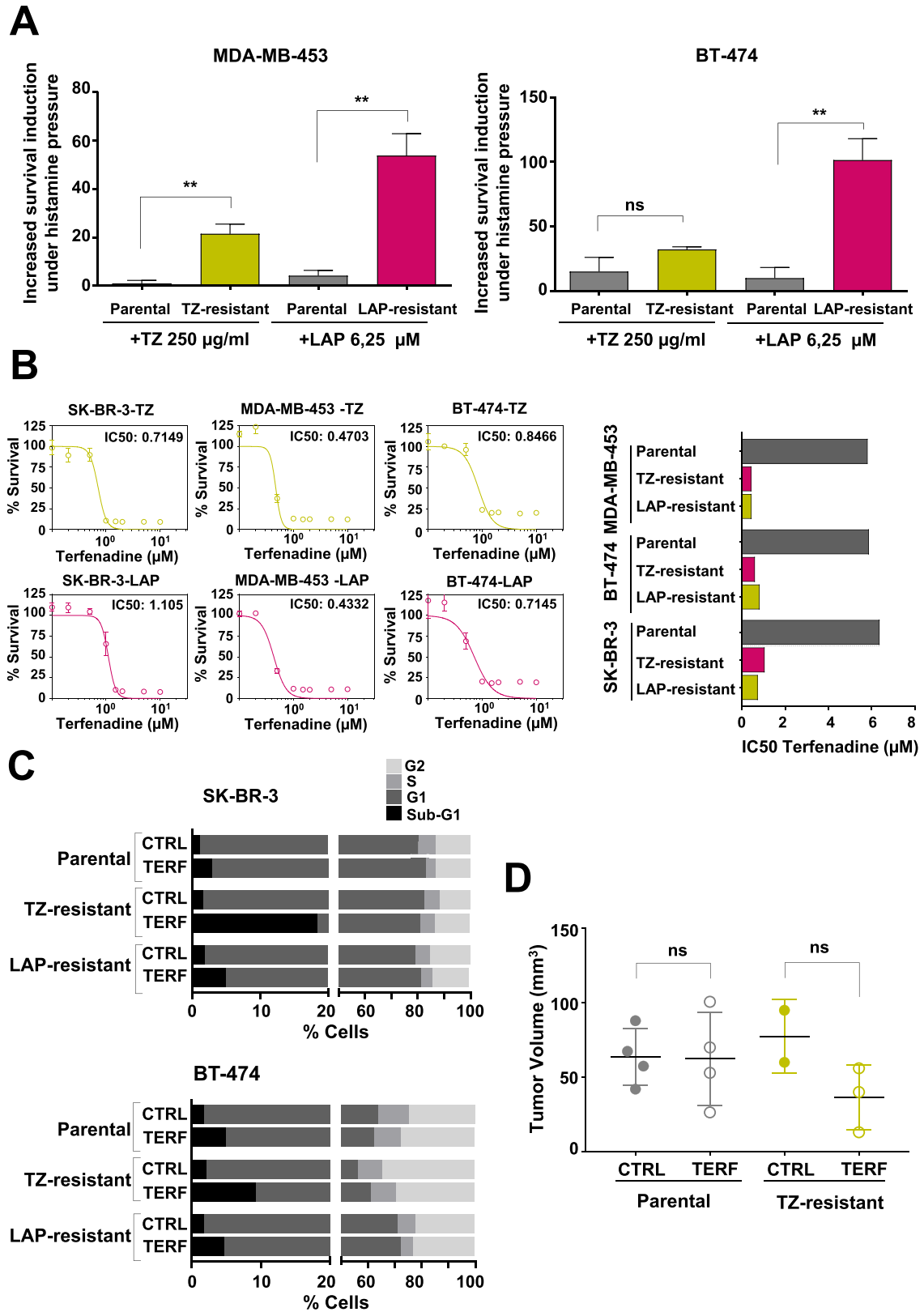


Fig. 6. Activation or inhibition effects of the HRH1 signaling pathway on HER2-targeted therapy-resistant BC survival.

(A) HER2-enriched parental and targeted therapy-resistant BC cell lines were pre-treated or not with 1 µM histamine for 6 h followed by treatment with increasing doses of trastuzumab (0–250 µg/ml) or lapatinib (0–6,25 µM) for 72 h. Graphical representation depicting the increment in survival of the cells pre-treated with histamine referred to the cells not pre-treated with histamine at the highest dose of trastuzumab (250 µg/ml) or lapatinib (6,25 µM). (B) Cell viability was evaluated in HER2-targeted therapy-resistant BC cell lines (SK-BR-3-TZ, SK-BR-3-LAP, MDA-MB-453-TZ, MDA-MB-453-LAP, BT-474-TZ, BT-474-LAP) using the MTT assay after treatment for 48 h with increasing doses of terfenadine treatment (0–10 µM) (left panels). The bars represent the mean IC50 (µM) of each BC cell line (right panel). Parental cell line IC50 values are depicted using data represented in Fig. 2A (left lower panel). (C) Graphic representation of SK-BR-3 and BT-474 (parental, trastuzumab and lapatinib resistant) cell cycle distribution in percentage values after treatment with vehicle or terfenadine (5 µM) for 48 h. (D) Tumor growth in orthotopically implanted MDA-MB-453 parental and trastuzumab cells treated daily intraperitoneally with vehicle (DMSO) or terfenadine (10 mg/kg) for 28 days. n = 4.

apoptosis, which is inhibited by U0126 (MEK1/2 inhibitor) or PD98059 [44] and, in oligodendroglial progenitor cells, ERK1/2 activation was reported to be responsible for IFN γ -induced death [45]. Although some authors have noted that HRH1 activation induces ERK1/2 phosphorylation [46], they have also described that it induces cytosolic restriction of pERK that enhances oxidative stress in cells, enlightening a novel signal transduction cascade associated with HRH1 activation that ends with apoptosis [46]. However, our results suggest that terfenadine induces apoptosis through ERK and p38 MAPK pathway activation in basal BC cells. The balance between pro-apoptotic and anti-apoptotic signals due to ERK1/2 activation and its subcellular location may regulate whether a cell proliferates or undergoes apoptosis. Although further research is needed to identify how these pathways are synchronized and their cross-talk in response to HRH1 inhibition, it is likely a new promising clinical target for basal and HER2-targeted therapy-resistant tumors.

Currently, standard treatments in neoadjuvant, adjuvant and metastatic settings for patients with HER2-enriched BC are mainly based on therapies, including trastuzumab and lapatinib [47]. However, even in cases with a complete clinical response, resistance lessens the success of treatment. Preventing resistance is essential to eradicate residual disease, and we suggest it might be accomplished by combining additional targeted therapies with anti-HER2 therapy. In a previous study, we demonstrated that HRH1 expression is higher in patients with HER2-enriched tumors [14]. In gastric cancer, HRH1 was found in circulating tumor cells [48] and could be used as a biomarker to predict which patients have minimal residual disease and, consequently, a higher risk of metastases. Moreover, in melanoma, HRH1 inhibition reduces tumor growth and avoids lung metastases [49]. Our results showed that HRH1 is overexpressed in trastuzumab- and lapatinib-resistant HER2 cell lines and that its activation by treatment with histamine specifically increased the viability of these BC resistant cells, suggesting resistant cells might be dependent on histamine-HRH1 signaling for survival.

Consistent with these findings, inhibition of HRH1 *in vivo* with terfenadine hampers MDA-MB-453 trastuzumab-resistant cell growth without affecting MDA-MB-453 parental cell growth, suggesting that HRH1 inhibition might sensitize HER2-targeted therapy-resistant cells to apoptosis. Although further studies are necessary to identify these mechanisms, to the best of our knowledge this is the first time that the HRH1 signaling pathway has been associated with HER2-enriched-subtype BC resistance and progression.

In conclusion, we identified HRH1 as a receptor frequently overexpressed in basal and HER2-targeted therapy-resistant BC cells, demonstrating that HRH1 inhibition culminates in apoptotic death and hampers tumor growth. We also identified ERK activation as the mechanism through which HRH1 blockade signals to promote death in basal BC cells. Our results provide a rationale for further investigation of anti-HRH1 therapies for basal BC tumors and combined anti-HER2 and anti-HRH1 therapies for HER2-enriched BC, as well as opens new lines in histamine pharmacology research. Thus, targeting HRH1 could directly contribute to advances in the treatment of poor-prognosis BC.

Conflicts of interest

The authors declare no potential conflicts of interest.

Funding

This work was sponsored by the Instituto de Salud Carlos III through the Plan Estatal de Investigación Científica y Técnica y de

Innovación, project reference number PI08022 and PI15/00661; This work was co-funded by the European Regional Development Fund (FEDER); the Fundación Cellex; Redes Temáticas de Investigación en Cáncer (RTICC, RD12/00360055); the Juan de la Cierva Fellowship program (GF; JCI-2011-10799); APIF fellowships from the University of Barcelona, School of Medicine (PFN, EE, ANC); Ayuda del Programa de Formación de Profesorado Universitario (FPU16/02744) (LRP); Sara Borrell Fellowship program (MM); Fundació per a la Recerca en Oncologia i Immunologia (FROI) (NM) and Beatriu de Pinós postdoctoral fellowship “AGAUR; BP-B 00160” (Co-funded by European Union) (PB). This work has been developed in a consolidated group by Secretaria d'Universitats i Recerca del Departament d'Economia i Coneixement (2014_SGR_530; 2017_SGR_1305).

Acknowledgments

This work was performed at IDIBAPS (CERCA Programme/Generalitat de Catalunya) and was developed at the building Centre de Recerca Biomèdica Cellex, Barcelona. We are particularly grateful to Darya Kulyk for image creation. We thank our colleagues R. Alonso and E. Ametller from the Laboratory of Molecular and Translational Oncology in Barcelona for their valuable assistance.

Appendix A. Supplementary data

Supplementary data related to this article can be found at <https://doi.org/10.1016/j.canlet.2018.03.014>.

References

- [1] J. Ferlay, I. Soerjomataram, R. Dikshit, S. Eser, C. Mathers, M. Rebelo, D.M. Parkin, D. Forman, F. Bray, Cancer incidence and mortality worldwide: sources, methods and major patterns in GLOBOCAN 2012, *Int. J. Canc.* 136 (2015) E359–E386.
- [2] R.L. Siegel, K.D. Miller, A. Jemal, *Cancer statistics, 2017*, *CA A Cancer J. Clin.* 67 (2017) 7–30.
- [3] C.M. Perou, T. Sorlie, M.B. Eisen, M. van de Rijn, S.S. Jeffrey, C.A. Rees, J.R. Pollack, D.T. Ross, H. Johnsen, L.A. Akslen, O. Fluge, A. Pergamenschikov, C. Williams, S.X. Zhu, P.E. Lonning, A.L. Borresen-Dale, P.O. Brown, D. Botstein, Molecular portraits of human breast tumours, *Nature* 406 (2000) 747–752.
- [4] A. Prat, J.S. Parker, O. Karginova, C. Fan, C. Livasy, J.I. Herschkowitz, X. He, C.M. Perou, Phenotypic and molecular characterization of the claudin-low intrinsic subtype of breast cancer, *Breast Cancer Res.* 12 (2014). R68.
- [5] D. Mendes, C. Alves, N. Afonso, F. Cardoso, J.L. Passos-Coelho, L. Costa, S. Andrade, F. Batel-Marques, The benefit of HER2-targeted therapies on overall survival of patients with metastatic HER2-positive breast cancer—a systematic review, *Breast Cancer Res.* 17 (2015) 140.
- [6] Z. Liu, X.S. Zhang, S. Zhang, Breast tumor subgroups reveal diverse clinical prognostic power, *Sci. Rep.* 4 (2014) 4002.
- [7] M.S. Mohd Shariq, J. Crown, B.T. Hennessy, Overcoming resistance and restoring sensitivity to HER2-targeted therapies in breast cancer, *Ann. Oncol.* 23 (2012) 3007–3016.
- [8] D.F. Quail, J.A. Joyce, Microenvironmental regulation of tumor progression and metastasis, *Nat. Med.* 19 (2013) 1423–1437.
- [9] P. Seifert, M. Spitznas, Tumours may be innervated, *Virchows Arch.* 438 (2001) 228–231.
- [10] B.S. Mitchell, U. Schumacher, E. Kaiserling, Are tumours innervated? Immunohistological investigations using antibodies against the neuronal marker protein gene product 9.5 (PGP 9.5) in benign, malignant and experimental tumours, *Tumor Biol.* 15 (1994) 269–274.
- [11] M. Kayahara, H. Nakagawara, H. Kitagawa, T. Ohta, The nature of neural invasion by pancreatic cancer, *Pancreas* 35 (2007) 218–223.
- [12] M. Mancino, E. Ametller, P. Gascon, V. Almdro, The neuronal influence on tumor progression, *Biochim. Biophys. Acta* 1816 (2011) 105–118.
- [13] K.S. Sastry, A.I. Chouchane, E. Wang, G. Kulik, F.M. Marincola, L. Chouchane, Cytoprotective effect of neuropeptides on cancer stem cells: vasoactive intestinal peptide-induced antiapoptotic signaling, *Cell Death Dis.* 8 (2017) e2844.
- [14] P. Fernandez-Nogueira, P. Bragado, V. Almdro, E. Ametller, J. Rios, S. Choudhury, M. Mancino, P. Gascon, Differential expression of neuropeptides among breast cancer subtypes identifies high risk patients, *Oncotarget* 7 (2016) 5313–5326.
- [15] S. Garcia-Recio, G. Fuster, P. Fernandez-Nogueira, E.M. Pastor-Arroyo, S.Y. Park, C. Mayordomo, E. Ametller, M. Mancino, X. Gonzalez-Farre,

- H.G. Russnes, P. Engel, D. Costamagna, P.L. Fernandez, P. Gascon, V. Almendro, Substance P autocrine signaling contributes to persistent HER2 activation that drives malignant progression and drug resistance in breast cancer, *Canc. Res.* 73 (2014) 6424–6434.
- [16] M. Amit, S. Na'ara, Z. Gil, Mechanisms of cancer dissemination along nerves, *Nat. Rev. Canc.* 16 (2016) 399–408.
- [17] C. Magnon, S.J. Hall, J. Lin, X. Xue, L. Gerber, S.J. Freedland, P.S. Frenette, Autonomic nerve development contributes to prostate cancer progression, *Science* 341 (2013) 1236361.
- [18] C.M. Zhao, Y. Hayakawa, Y. Kodama, S. Muthupalani, C.B. Westphalen, G.T. Andersen, A. Flatberg, H. Johannessen, R.A. Friedman, B.W. Renz, A.K. Sandvik, V. Beisvag, H. Tomita, A. Hara, M. Quante, Z. Li, M.D. Gershon, K. Kaneko, J.G. Fox, T.C. Wang, D. Chen, Denervation suppresses gastric tumorigenesis, *Sci. Transl. Med.* 6 (2014), 250ra115.
- [19] M. Wang, X. Wei, L. Shi, B. Chen, G. Zhao, H. Yang, Integrative genomic analyses of the histamine H1 receptor and its role in cancer prediction, *Int. J. Mol. Med.* 33 (2014) 1019–1026.
- [20] E.S. Rivera, G.P. Cricco, N.I. Engel, C.P. Fitzsimons, G.A. Martin, R.M. Bergoc, Histamine as an autocrine growth factor: an unusual role for a widespread mediator, *Semin. Canc. Biol.* 10 (2000) 15–23.
- [21] G. Cricco, G. Martin, V. Medina, M. Nunez, A. Gutierrez, C. Cocca, R. Bergoc, E. Rivera, Histamine regulates the MAPK pathway via the H(2) receptor in PANC-1 human cells, *Inflamm. Res.* 53 (Suppl 1) (2004) S65–S66.
- [22] C. Davio, A. Baldi, A. Mladovan, G. Cricco, C. Fitzsimons, R. Bergoc, E. Rivera, Expression of histamine receptors in different cell lines derived from mammary gland and human breast carcinomas, *Inflamm. Res.* 44 (Suppl 1) (1995) S70–S71.
- [23] A. Patel, V. Vasanthan, W. Fu, R.P. Fahlman, D. MacTavish, J.H. Jhamandas, Histamine induces the production of matrix metalloproteinase-9 in human astrocytic cultures via H1-receptor subtype, *Brain Struct. Funct.* 221 (2015) 1845–1860.
- [24] S. Higuchi, A. Tanimoto, N. Arima, H. Xu, Y. Murata, T. Hamada, K. Makishima, Y. Sasaguri, Effects of histamine and interleukin-4 synthesized in arterial intima on phagocytosis by monocytes/macrophages in relation to atherosclerosis, *FEBS Lett.* 505 (2001) 217–222.
- [25] A. Arachiche, I. Badirou, J. Dachary-Prigent, I. Garcin, D. Geldwerth-Feniger, D. Kerbiriou-Nabias, ERK activation by Ca²⁺ ionophores depends on Ca²⁺ entry in lymphocytes but not in platelets, and does not conduct membrane scrambling, *Cell. Mol. Life Sci.* 65 (2008) 3861–3871.
- [26] P. Rafferty, S.T. Holgate, Terfenadine (Seldane) is a potent and selective histamine H1 receptor antagonist in asthmatic airways, *Am. Rev. Respir. Dis.* 135 (1987) 181–184.
- [27] E. Hadzijušufovic, B. Peter, K.V. Gleixner, K. Schuch, W.F. Pickl, T. Thaiwong, V. Yuzbasiyan-Gurkan, I. Mirkina, M. Willmann, P. Valent, H1-receptor antagonists terfenadine and loratadine inhibit spontaneous growth of neoplastic mast cells, *Exp. Hematol.* 38 (2010) 896–907.
- [28] F. Nicolau-Galmes, A. Asumendi, E. Alonso-Tejerina, G. Perez-Yarza, S.M. Jangi, J. Gardeazabal, Y. Arroyo-Berdugo, J.M. Careaga, J.L. Diaz-Ramon, A. Apraiz, M.D. Boyano, Terfenadine induces apoptosis and autophagy in melanoma cells through ROS-dependent and -independent mechanisms, *Apoptosis* 16 (2011) 1253–1267.
- [29] N. Inagaki, K. Igeta, J.F. Kim, M. Nagao, N. Shiraishi, N. Nakamura, H. Nagai, Involvement of unique mechanisms in the induction of scratching behavior in BALB/c mice by compound 48/80, *Eur. J. Pharmacol.* 448 (2002) 175–183.
- [30] R.M. Neve, K. Chin, J. Fridlyand, J. Yeh, F.L. Baehner, T. Fevr, L. Clark, N. Bayani, J.P. Coppe, F. Tong, T. Speed, P.T. Spellman, S. DeVries, A. Lapuk, N.J. Wang, W.L. Kuo, J.L. Stilwell, D. Pinkel, D.G. Albertson, F.M. Waldman, F. McCormick, R.B. Dickson, M.D. Johnson, M. Lippman, S. Ethier, A. Gazdar, J.W. Gray, A collection of breast cancer cell lines for the study of functionally distinct cancer subtypes, *Canc. Cell* 10 (2006) 515–527.
- [31] G.P. Cricco, C.A. Davio, G. Martin, N. Engel, C.P. Fitzsimons, R.M. Bergoc, E.S. Rivera, Histamine as an autocrine growth factor in experimental mammary carcinomas, *Agents Actions* 43 (1994) 17–20.
- [32] S. Lamouille, J. Xu, R. Derynck, Molecular mechanisms of epithelial-mesenchymal transition, *Nat. Rev. Mol. Cell Biol.* 15 (2014) 178–196.
- [33] J.D. Liu, Y.J. Wang, C.H. Chen, C.F. Yu, L.C. Chen, J.K. Lin, Y.C. Liang, S.Y. Lin, Y.S. Ho, Molecular mechanisms of G0/G1 cell-cycle arrest and apoptosis induced by terfenadine in human cancer cells, *Mol. Carcinog.* 37 (2003) 39–50.
- [34] C. Chen, G. Li, W. Liao, J. Wu, L. Liu, D. Ma, J. Zhou, R.H. Elbekai, M.L. Edin, D.C. Zeldin, D.W. Wang, Selective inhibitors of CYP2J2 related to terfenadine exhibit strong activity against human cancers in vitro and in vivo, *J. Pharmacol. Exp. Therapeut.* 329 (2009) 908–918.
- [35] W.T. Wang, Y.H. Chen, J.L. Hsu, W.J. Leu, C.C. Yu, S.H. Chan, Y.F. Ho, L.C. Hsu, J.H. Guh, Terfenadine induces anti-proliferative and apoptotic activities in human hormone-refractory prostate cancer through histamine receptor-independent Mcl-1 cleavage and Bak up-regulation, *Naunyn-Schmiedeberg's Arch. Pharmacol.* 387 (2014) 33–45.
- [36] S.M. Jangi, J.L. Diaz-Perez, B. Ochoa-Lizarralde, I. Martin-Ruiz, A. Asumendi, G. Perez-Yarza, J. Gardeazabal, J.L. Diaz-Ramon, M.D. Boyano, H1 histamine receptor antagonists induce genotoxic and caspase-2-dependent apoptosis in human melanoma cells, *Carcinogenesis* 27 (2006) 1787–1796.
- [37] S.M. Jangi, M.B. Ruiz-Larrea, F. Nicolau-Galmes, N. Andollo, Y. Arroyo-Berdugo, I. Ortega-Martinez, J.L. Diaz-Perez, M.D. Boyano, Terfenadine-induced apoptosis in human melanoma cells is mediated through Ca²⁺ homeostasis modulation and tyrosine kinase activity, independently of H1 histamine receptors, *Carcinogenesis* 29 (2008) 500–509.
- [38] R. Enomoto, T. Komai, Y. Yoshida, C. Sugahara, E. Kawaguchi, K. Okazaki, H. Kinoshita, H. Komatsu, Y. Konishi, E. Lee, Terfenadine induces thymocyte apoptosis via mitochondrial pathway, *Eur. J. Pharmacol.* 496 (2004) 11–21.
- [39] T.F. Franke, C.P. Hornik, L. Segev, G.A. Shostak, C. Sugimoto, PI3K/Akt and apoptosis: size matters, *Oncogene* 22 (2003) 8983–8998.
- [40] A.S. Dhillon, S. Hagan, O. Rath, W. Kolch, MAP kinase signalling pathways in cancer, *Oncogene* 26 (2007) 3279–3290.
- [41] J.M. Kyriakis, J. Avruch, Mammalian mitogen-activated protein kinase signal transduction pathways activated by stress and inflammation, *Physiol. Rev.* 81 (2001) 807–869.
- [42] C.R. Weston, R.J. Davis, The JNK signal transduction pathway, *Curr. Opin. Cell Biol.* 19 (2007) 142–149.
- [43] Y. Mebratu, Y. Tesfagzi, How ERK1/2 activation controls cell proliferation and cell death: is subcellular localization the answer? *Cell Cycle* 8 (2009) 1168–1175.
- [44] D. Sinha, S. Bannerjee, J.H. Schwartz, W. Lieberthal, J.S. Levine, Inhibition of ligand-independent ERK1/2 activity in kidney proximal tubular cells deprived of soluble survival factors up-regulates Akt and prevents apoptosis, *J. Biol. Chem.* 279 (2004) 10962–10972.
- [45] M. Horiuchi, A. Itoh, D. Pleasure, T. Itoh, MEK-ERK signaling is involved in interferon-gamma-induced death of oligodendroglial progenitor cells, *J. Biol. Chem.* 281 (2006) 20095–20106.
- [46] R. Jain, U. Watson, D.K. Saini, ERK activated by Histamine H1 receptor is anti-proliferative through spatial restriction in the cytosol, *Eur. J. Cell Biol.* 95 (2016) 623–634.
- [47] F.J. Esteva, D. Yu, M.C. Hung, G.N. Hortobagyi, Molecular predictors of response to trastuzumab and lapatinib in breast cancer, *Nat. Rev. Clin. Oncol.* 7 (2010) 98–107.
- [48] N. Matsumura, H. Zembutsu, K. Yamaguchi, K. Sasaki, T. Tsuruma, T. Nishidate, R. Denno, K. Hirata, Identification of novel molecular markers for detection of gastric cancer cells in the peripheral blood circulation using genome-wide microarray analysis, *Exp. Ther. Med.* 2 (2011) 705–713.
- [49] B. Blaya, F. Nicolau-Galmes, S.M. Jangi, I. Ortega-Martinez, E. Alonso-Tejerina, J. Burgos-Bretones, G. Perez-Yarza, A. Asumendi, M.D. Boyano, Histamine and histamine receptor antagonists in cancer biology, *Inflamm. Allergy - Drug Targets* 9 (2010) 146–157.